Research on Application of Multi-Physical Coupling Model in Prediction and Control of Surface Subsidence in Coal Mining

Meng Huang¹, Xingyao Zhou², *, Chao Ju¹, and Chenghao Ning¹

¹ China Energy Technology & Economics Research Institute, Beijing 100000, China ² China National Institute of Standardization, Beijing 100000, China *Corresponding author

Abstract:

Addressing the issue of terrain depression stemming from coal extraction, this investigation delves into the utility of a multiphysics integration model for forecasting and managing subsidence phenomena. The impact of coal excavation operations on the surface configuration is a sophisticated amalgamation of multi-physics field interactions, encompassing the interplay of pressure, fluid dynamics, thermal conditions, and additional physical domains. Through the strategic design of algorithms, the system achieves a high level of precision in terrain depression prediction. Simulation outcomes reveal a pronounced non-linear correlation between terrain depression and pivotal factors like excavation depth, rate of extraction, and the expanse of the mining zone, under specified mining circumstances. Statistical evaluation indicates that the accuracy in predicting terrain depression surpasses 97%, with the margin of error maintained under 3%. Moreover, this treatise scrutinizes the repercussions of varying mining tactics on terrain depression, uncovering that through the refinement of mining variables, terrain depression can be efficiently curtailed, thus mitigating the adverse impacts on the natural habitat. This inquiry not only furnishes a theoretical foundation for the prediction of terrain depression in the context of coal mining, but also offers technical directives and a pragmatic pathway towards implementing eco-friendly mining practices and safeguarding the environment, bearing considerable practical importance and applicability for the enduring progress of the coal sector.

Keywords: Multi-physics coupling model; Coal mining; Surface subsidence; Bertalanffy time function.

INTRODUCTION

As an important energy resource, coal plays an irreplaceable role in the country's economic development. However, coal mining activities inevitably affect the surface structure and cause surface subsidence, which not only threatens the safety of surface buildings, but also may damage the ecological environment. Therefore, accurately predicting and effectively controlling surface subsidence caused by coal mining has become a key issue for the sustainable development of the coal industry. Traditional mine mining methods often lead to environmental disasters such as ground collapse, which seriously damages the ecological balance. Conventional coal mining technology relies on manual underground operations, and requires huge investments in equipment purchase and surface operations in the early stage, with significant safety risks. For Chinese unique "three down and up" coal seams, that is, under buildings, under water bodies, under railways, and on pressurized water bodies, traditional mining methods require huge amounts of money to relocate residents, which undoubtedly reduces the economic benefits of the mining area. Underground coal gasification technology, by inducing a series of thermochemical changes deep in the stratum, eliminates the construction of underground transportation systems and ground facilities, directly seals waste such as gangue in situ, effectively alleviates the problem of gangue mountain accumulation, and has a significant effect on reducing environmental pollution after coal mining. The introduction of underground coal gasification technology transforms the traditional mechanical coal mining process into a thermochemical reaction, which greatly reduces the mining cost and significantly improves the economic benefits of the mining area. With the help of underground coal gasification technology, the coal resources left over from conventional mining can be recovered, which is particularly suitable for the "three down and one up" coal seams, thin coal seams and deep coal seams that are difficult to reach or have low economic benefits.

As an innovative coal mining technology, underground coal gasification is mainly carried out underground with low human intervention. In addition, Chinese geological structure is complex and there are significant differences between the east and the west, so it faces many challenges. This is the essential difference from traditional underground mining. In recent years, the multiphysics field coupling model has become a powerful tool for studying surface subsidence in coal mining because it can comprehensively consider the interaction of multiple physical fields such as stress, fluid, and temperature in the mining process. As a mathematical model that describes biological growth, the nonlinear characteristics of the Bertalanffy time function have also been introduced into the prediction of surface subsidence to simulate the nonlinear law of surface subsidence changing with time.

Reference [1] proposed a multi-physics coupling model based on Bertalanffy time function. The model considers the nonlinear effect of time on surface subsidence and solves the problem of reduced accuracy of traditional models in long-term prediction. Reference [2] further incorporates the coupling effect of groundwater flow and surface subsidence into the model, reveals the mechanism of the influence of groundwater level change on surface subsidence, and provides theoretical support for the protection of hydrogeological environment in coal mining areas.

Reference [3] uses finite element analysis technology to construct a multi-physics coupling model. By dynamically simulating the stress and strain of the formation before and after mining, it realizes the real-time prediction of surface subsidence and significantly improves the prediction accuracy and reliability. Reference [4] proposes a mining scheme optimization method based on a multi-physics coupling model from the perspective of surface subsidence control. By adjusting the mining sequence and mining parameters, it effectively reduces the impact of mining on the surface environment and provides a new idea for realizing green mining.

References [5] and [6] discuss how to improve the applicability and reliability of multi-physics coupling models from the perspectives of parameter identification and uncertainty analysis, respectively. Reference [5] proposed a parameter inversion method based on machine learning. By training the model, the nonlinear relationship between formation parameters and surface subsidence was automatically learned, thereby improving the prediction accuracy of the model. Reference [6] introduced the Monte Carlo method to perform uncertainty analysis on the prediction results of the model, providing decision makers with more comprehensive and objective information.

References [7] and [8] focus on the computational efficiency and scope of application of the model. Reference [7] developed a multi-physics coupling method based on an agent model, which made large-scale surface subsidence prediction possible by reducing the computational cost. Reference [8] proposed a multi-scale multi-physics coupling model suitable for complex geological conditions, solving the problem of the applicability of traditional models in complex geological environments.

Reference [9] and [10] focus on the verification and application of the model. Reference [9] verified the effectiveness and accuracy of the multi-physics coupling model in surface subsidence prediction by comparing field monitoring data with simulation results. Reference [10] proposed a set of engineering practice solutions for surface subsidence control based on a multi-physics field coupling model, providing a specific operational guide for environmental management in coal mining areas.

This paper aims to construct a multi-physics field coupling model, combined with the Bertalanffy time function, to achieve accurate prediction of surface subsidence in coal mining. Through algorithm design and simulation analysis, this paper will deeply explore the prediction ability and optimization strategy of the model to provide a scientific basis for mining decision-making in the coal industry. At the same time, this paper will also study surface subsidence control technology, explore how to minimize the impact on the environment while ensuring coal mining efficiency, achieve harmonious coexistence of mining activities and environmental protection, and contribute wisdom and strength to the sustainable development of the coal industry.

SURFACE SUBSIDENCE MECHANISM OF UNDERGROUND COAL GASIFICATION

The underground coal gasification procedure encompasses an ensemble of thermally-driven chemical transformations, effectuating controlled coal combustion, immobilizing byproducts like cinder and shale within the combustion zone, and subsequently generating an abundance of combustible gases. Shaftless underground coal gasification technology harnesses directional drilling to establish gas supply and extraction conduits, igniting and initiating coal combustion, with all operations executed at the surface level, thus making it challenging to directly and accurately visualize and gauge the morphology of the post-gasification residue area. Grasping the geometric attributes of the residue area post shaftless underground coal gasification is the cornerstone for simulating the movement dynamics of the overlaying strata. Therefore, this study meticulously references pertinent literature, adopting a synergistic approach combining mathematical modeling and theoretical analysis, grounded in a detailed dissection of the transport network, stratigraphic configuration, and coal seam dispersion within the experimental zone. This approach yields the configuration of the residue area and the structure of the coal rib post completion of ideal shaftless dual-channel underground coal gasification; further, it explores the fluctuation range of the rock mass's physical-mechanical parameters under the high-temperature effect of the shaftless dual-channel underground coal gasification.

The arrangement of the operation zone in the retroactively controlled gas injection underground gasification process mirrors that of standard strip mining, namely, executing a single gasification operation and preserving a segment of coal to ensure gasification operational safety and govern the propagation of fractures in the overlaying strata. Nonetheless, during the underground coal gasification process, the temperature within the surrounding rock in the depleted zone might soar beyond 1000 degrees Celsius, not only triggering thermal stress but also altering the mechanical attributes of the surrounding rock, engendering a high-

temperature impact on the surrounding rock within the depleted zone. Coupled with the distinctiveness of the underground coal gasification process, the contour of the gasification operation zone starkly diverges from the rectangular operation zone of traditional underground mining. Moreover, gasification byproducts like solid residues such as ash will remain in the depleted zone, precipitating marked contrasts in the deformation of the surrounding rock between underground coal gasification and strip mining. In general, there are significant disparities in the characteristics of surrounding rock fractures between underground coal gasification and conventional strip mining, but both can engender fractures of a specific elevation. As deformation ascends upward, the actual tensile force exerted on the rock will be inferior to its ultimate tensile strength at a certain level. At this juncture, the upper stratum will undergo comprehensive, continuous bending deformation, precipitating coordinated subsidence of the overlaying layer, which will then be transmitted to the surface, culminating in surface displacement and deformation (Figure 1 adapted from Void fraction distribution in overburden disturbed by longwall mining of coal). Hence, the bending deformation of the overlaying strata instigated by the gasification operation area will induce surface subsidence. Furthermore, given the necessity to preserve the isolated coal body during the underground coal gasification process, when the operation area is gasified and the depleted zone cannot uphold the overlaying load, the overlaying strata's load will be borne by the isolated coal body, resulting in compressive deformation of the coal body. Simultaneously, under the sway of gasification disturbance, the coal bodies flanking the depleted zone will become more susceptible to yield and soften, and the bearing capacity of the yield zone of the coal body will be diminished, exacerbating the compressive deformation of the elastic zone of the coal body. Compressive deformation in the yield zone and elastic zone of the coal body will instigate coordinated subsidence of the overlaying strata, further amplifying surface subsidence. The root cause of surface subsidence instigated by underground coal gasification is the bending deformation of the overlaying strata and the compressive deformation of the isolated coal body. Consequently, surface subsidence can be forecast by computing the bending value of the overlaying strata and the compression of the isolated coal body.

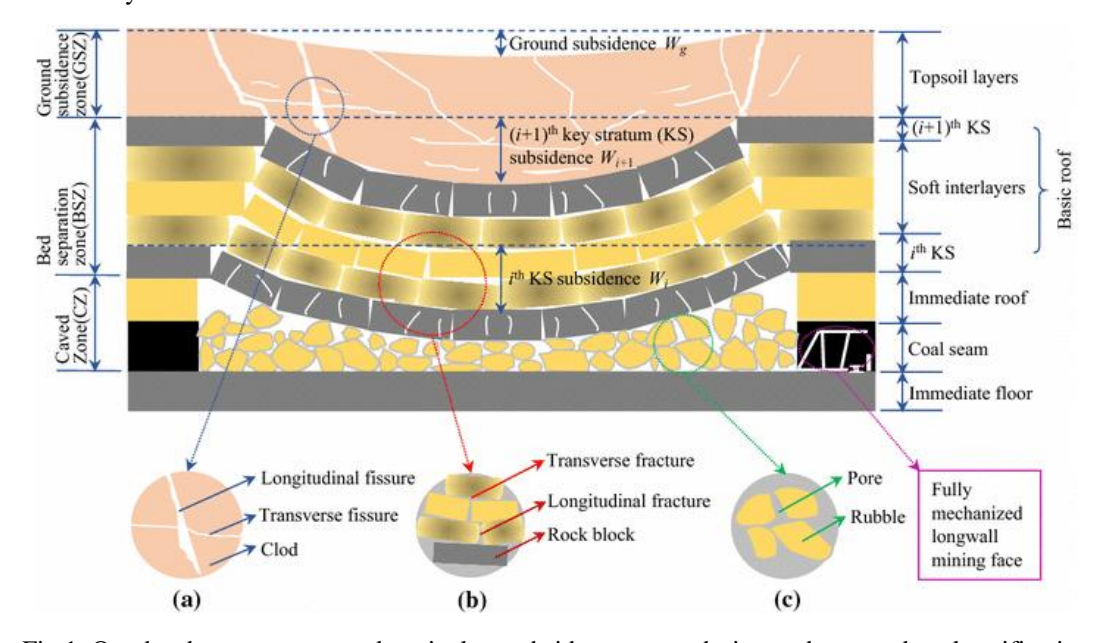


Fig.1. Overburden movement and equivalent subsidence space during underground coal gasification

SURFACE DYNAMIC SUBSIDENCE PREDICTION MODEL

MMF model was proposed in 1975 as an "S-shaped" growth curve model, which was used by Wang Junbao et al. in the prediction of surface subsidence time.

$$\lambda(k) = \lambda_m \frac{k^{\beta}}{\gamma + k^{\beta}} \tag{1}$$

 γ, β is a time-influenced parameter, which is related to the lithology of overlying rock in stope. The first and second order functions of the function are derived, and the functions of the subsidence velocity $u(k) = \lambda_m \beta \gamma k^{\beta-1}/(\gamma + k^{\beta})^2$ and subsidence acceleration $\alpha(k) = \lambda_m \beta \gamma k^{\beta-2} (\beta \alpha - \gamma - \beta k^{\beta} - k^{\beta})/(\gamma + k^{\beta})^3$ are analyzed [11]. The physical significance

of β and γ remains to be studied. Neither the sinking velocity nor the acceleration can be expressed in time k=0. The time function established by Sroka based on Knothe function is

$$G_{Sroka}(k) = 1 + \frac{\delta}{1 - g} e^{-gk} - \frac{g}{g - \delta} e^{-gk}$$
 (2)

g is the relative convergence rate of rock strata. δ is the time coefficient of the overlying strata, which is used to describe the hysteresis effect of the strata. The function has the following characteristics: The curve of the function is not S-type. The sinking velocity is closer to the ideal time function, but the shape of the sinking acceleration curve is incorrect [12]. In practical application, g and δ are not existing parameters, and the parameters are difficult to obtain, and g and g are difficult to find at the same time. VonBertalanffy model is a common biological growth model, mainly used to predict the growth of plants and animals, and is often used in economics and statistics. This model is a generalization of Logistic and has good flexibility. Its function equation is

$$\lambda(k) = \lambda_m (1 - \beta e^{-\gamma k})^3 \tag{3}$$

In the formula, β and γ are time-influenced parameters, where β can reflect the initial settlement value at k=0, and γ reflects the initial settlement acceleration value at k=0. Considering the nonlinearities of rock strata and surface movement, especially for full-mechanized caving mining of ultra-thick coal seam near shallow buried depth, concentrated surface subsidence deformation and steep basin edge, the 3rd power of Bertalanffy function is changed into a time-influenced parameter ζ , which is used in the study of dynamic surface subsidence in coal mining [13]. The Bertalanffy function can be improved to a three-parameter model:

$$\lambda(k) = \lambda_m (1 - \beta e^{-\gamma k})^{\zeta} \tag{4}$$

Parameter γ is the initial settlement velocity parameter, and parameter ζ is the curve shape parameter. In order to further study the applicability of this model in coal mining subsidence prediction, the first and second order functions of this function are derived.

$$u(k) = \lambda_m \beta \gamma \zeta (1 - \beta e^{-\gamma k})^{\zeta - 1} e^{-\gamma k}$$
(5)

$$\alpha(k) = \lambda_m \beta \gamma^2 \zeta e^{-\gamma k} (1 - \beta e^{-\gamma k})^{\zeta - 2} (\beta \zeta e^{-\gamma k} - 1)$$
 (6)

The dynamic subsidence, subsidence velocity and subsidence acceleration time functions of improved Bertalanffy three-parameter time function have the following characteristics:

- (1) Monotonicity. Since the parameters β , γ and ζ are both positive, $(1 \beta e^{-\gamma k})^{\zeta} > 0$, $\lambda(k)$ is an increasing function of k.
- (2) concavity. Let $\lambda''(k) = \alpha(k) = 0$, find the time coordinate of the inflection point $k = \ln(\beta \zeta)/\gamma$, then $\lambda(k_0) = \lambda_m (1-1/\zeta)^{\zeta}$, and when $k < k_0$, the subsidence curve is "concave", when $k > k_0$, the subsidence curve is "convex". That is, $\lambda(k)$ is the "S-shaped" curve of time k.
- (3) Gradualism. Is A bounded function with an asymptote of $\lambda(k) = \lambda_m$.

EXAMPLE APPLICATION

Overview of the study area

The gasification technology used is the "belt mining and surface mining" gasifier reverse-controlled gas-filled underground gasification method, which is the world's leading technology. Four gasification working areas and three spacer coal bodies are planned [14]. The average depth of underground coal gasification operation area is 285.65 meters. The thickness of the coal seam is 5.6 meters, and the coal in this layer mainly belongs to the brown coal category. The gasification cycle of a single operation

area is 99 days, forming a post-gasification burning area with a length of 175 meters and a width of 17.5 meters. Four gasification operation areas are designed, and coal bodies with a width of 25.5 meters are reserved for each operation area as isolation (FIG. 2).

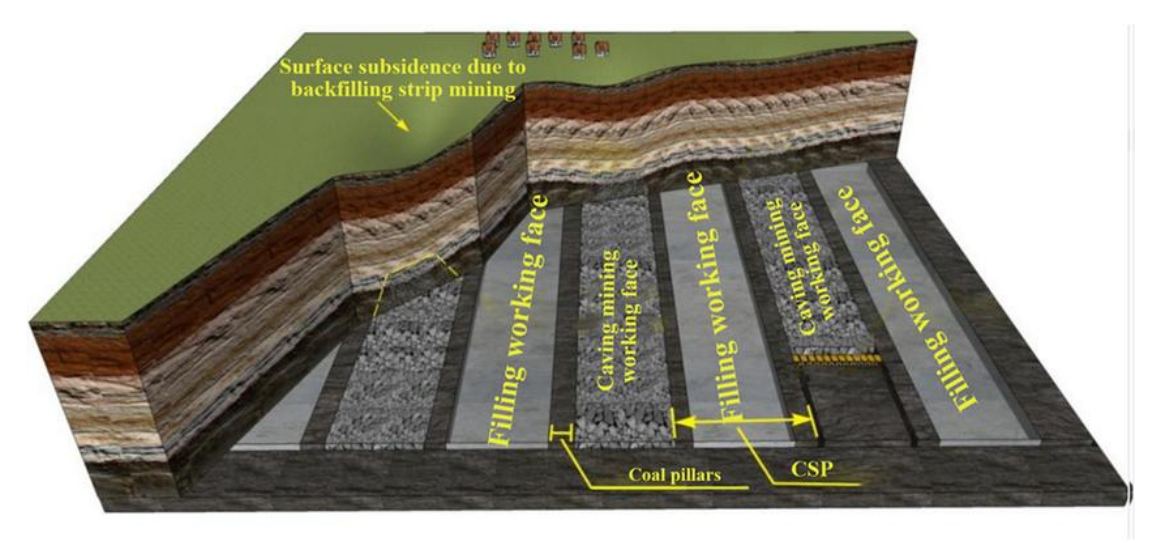


Fig.2. Schematic diagram of gas-filled underground gasification process under reverse control of "strip mining - surface mining" gasifier.

Rock fracture identification and buckling deformation estimation

The overlying rock structure and rock mechanical properties of the underground coal gasification experiment area are detailed in Table 1.

lithology	Thickness /m	Poisson's ratio	Mean gravity density/(kg·m3)	Tensile strength /MPa
siltstone	16	0.27	2297	1.17
mudstone	2	0.29	2236	0.86
siltstone	1	0.27	2297	1.17
mudstone	9	0.29	2236	0.86
siltstone	2	0.27	2297	1.17
mudstone	2	0.29	2236	0.86
Fine grained sandstone	1	0.33	2407	0.86
mudstone	4	0.29	2236	0.86
Fine grained sandstone	1	0.33	2407	0.86
mudstone	5	0.29	2236	0.86
Coal seam	3	0.24	1458	0.52
mudstone	3	0.29	2236	0.86
Sandy mudstone	1	0.26	2413	0.74
Sandy mudstone	3	0.26	2413	0.74
mudstone	4	0.29	2236	0.86
Coal seam	5	0.24	1458	0.52

Table 1. Distribution of rock strata and its mechanical parameters.

The Laplace transform calculation of temperature field is complicated, and the conduction range of temperature field to overburden is very limited. In the calculation of temperature field conduction, the overlying layer can be simplified to 12 meters thick muddy layer and 17 meters thick sandy layer. Set the temperature value of the heat source to 1000 degrees Celsius; The ground temperature of the original rock is 26.5° C, and the thermophysical properties of the rock are listed in Table 2.

Table 2. Thermophysical parameters of rock strata.
--

lithology	Thermal conductivity /(W•m-1•K-1)	Specific Heat Capacity c/(J•kg-1•K-1)	Time t/s	Density /(kg•m-3)	Thermal diffusion coefficient a/(m2•s-1)
mudstone	1.25	927	8100000	2413	5.963×10-7
sandstone	1.25	1052	8100000	2297	5.593×10-7

The calculation results show that the 5.6m thick argillaceous layer is not fractured, but it cannot bear all the load of the overlying rock, and the number of fractured layers is 5. The silty sand layer of 16.5 meters thick can support the load of the overlying rock, which will restrict the displacement and deformation of the overlying rock. Through calculation, the maximum bending deformation of this silty sandy layer is 14.32 cm, and the three-dimensional bending morphology of the rock layer is shown in Figure 3.

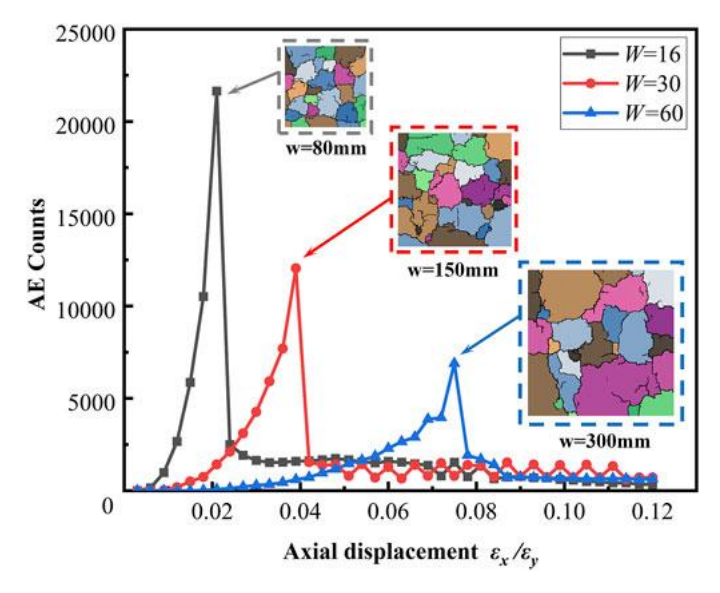


Fig. 3. Three-dimensional flexure of rock mass.

Assessment of maximum shrinkage of gasification coal pillar

The thermal physical properties of coal column include: heat source temperature 1000° C, initial temperature of the original rock layer 24°C, thermal conductivity 0.75W/(m·K), specific heat capacity 1578J/(kg·K), time t 5195000 seconds, density 1700kg/m³, thermal diffusion coefficient 9.81×10^{-8} m²/s.

Upon the conclusion of the underground coal gasification operation, the coal undergoes combustion to create a combustion sector. The adjacent rock mass forfeits the coal's support, leading to a disruption of the initial stress equilibrium. Stress is then redistributed, culminating in the establishment of a new balance. Under the influence of elevated temperatures, the mechanical characteristics of the protective coal pillar undergo alteration. Bearing the weight of the overlaying strata, the coal pillar yields to a certain extent, engendering a specific-width plastic deformation area. In the context of numerical simulation analysis, the distribution attributes of the plastic deformation area vividly mirror the load-bearing efficacy of the protective coal pillar postunderground coal gasification, facilitating a more direct and efficacious assessment of the coal pillar's support capability. As illustrated in Figure 4, the roof subsidence curves of all numerical simulation models exhibit undulating patterns, with peaks precisely above the combustion void region. When both the combustion void area's width and the protective coal pillar's width remain unaltered, and the combustion void area's height ascends from 3 meters to 4, 5, 6, 7, and 8 meters, the maximal subsidence increments of the two contiguous models' roofs are 6 millimeters, 14 millimeters, 19 millimeters, 49 millimeters, and 15 millimeters, respectively. As the combustion void area's height escalates, the increase in the maximal roof subsidence value demonstrates a trajectory of initial gradual rise, followed by a sudden leap, and subsequently a deceleration. This is attributed to the fact that when the combustion void area's height reaches 7 meters, the ultimate load capacity on either side of the "inverted trapezoidal" protective coal pillar under the high-temperature effect is surpassed. This might instigate the collapse or failure of the coal walls on either side, transforming the inverted trapezoidal protective coal pillar into a virtually rectangular coal pillar to shoulder the burden of the superimposed strata. Consequently, the upward trend of the roof subsidence value becomes less pronounced.

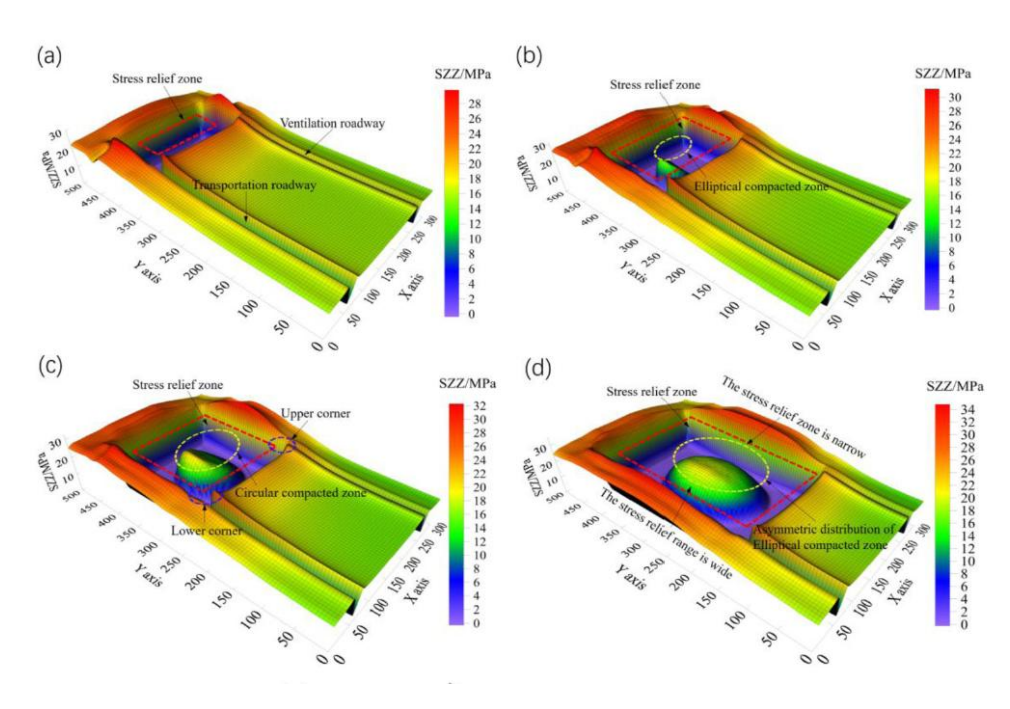


Fig. 4. Comparison of vertical stress in roof

When the expanse of the combustion sector is anchored at 12 meters, the breadth of the segregated coal rib escalates from 12 meters to 20 meters, 28 meters, and 36 meters, and the zenith vertical stress values of the two contiguous models atop the segregated coal rib diminish by 1.74 MPa, augment by 0.36 MPa, and swell by 0.25 MPa, respectively [15]; when the expanse of the combustion sector is stabilized at 20 meters, the breadth of the segregated coal rib amplifies from 12 meters to 20 meters, 28 meters, and 36 meters, and the zenith vertical stress values of the two contiguous models atop the segregated coal rib dwindle by 0.48 MPa, surge by 0.33 MPa, and climb by 0.42 MPa, respectively; when the expanse of the combustion sector is fixed at 28 meters, the breadth of the segregated coal rib grows from 12 meters to 20 meters, 28 meters, and 36 meters, and the zenith vertical stress values of the two contiguous models atop the segregated coal rib dwindle by 1.82 MPa, surge by 0.13 MPa, and climb by 0.09 MPa, respectively. When the expanse of the combustion void sector persists unchanged and the architecture of the segregated coal rib is steadfast, the zenith vertical stress is predominantly concentrated in the ceiling region above the segregated coal rib; the vertical stress value of the ceiling ascends and then descends with the augmentation of the width of the segregated coal rib. When the expanse of the combustion void sector is congruent to the breadth of the segregated coal rib, the zenith vertical stress is concentrated in the ceiling position above the segregated coal rib. When the altitude of the combustion void sector amplifies from 3 meters to 4 meters, 5 meters, 6 meters, 7 meters, and 8 meters, the zenith vertical stress of the ceiling exhibits a slight ascent, yet the increase is inconsequential [16]. This stems from the fact that when the breadth of the segregated coal rib is 28 meters, the coal rib boasts superior stability and can efficaciously uphold the stratum above. When the expanse of the combustion void sector is anchored, as the breadth of the isolation coal rib progressively escalates, the ratio of the plastic deformation sector of the isolation coal rib progressively dwindles, and the plastic deformation sector is predominantly concentrated on the coal ribs flanking the combustion void sector; when the breadth of the isolation coal rib is 12 meters, the isolation coal rib has been utterly metamorphosed into a plastic deformation sector, devoid of an elastic core sector, signifying that the isolation coal rib established at this juncture has become unstable and is incapable of upholding the upper stratum; when the breadth of the isolation coal rib amplifies to 20 meters, 28 meters, and 36 meters respectively, an elastic core sector materializes in the isolation coal rib, and as the breadth of the isolation coal rib amplifies, the ratio of the elastic core sector progressively swells, indicating that the isolation coal rib at this juncture can uphold the upper stratum and its stability progressively ascends.

Prediction of ground settlement in the experimental area

Displayed in Figure 5 is the topographic map depicting surface subsidence. At CG05 monitoring station, within the experimental zone, the surface subsidence measures 42 millimeters, positioned ten meters distant from the working face's central line. The recently devised methodology aligns seamlessly with empirical observations. Contrasted with the extant technique for predicting surface subsidence, which hinges on "actual mining thickness", the zenith subsidence value is 96 millimeters. This forecast is

notably more precise and can cater more proficiently to the technical requisites for salvaging "three down" coal reserves, which pose challenges for conventional underground mining endeavors.

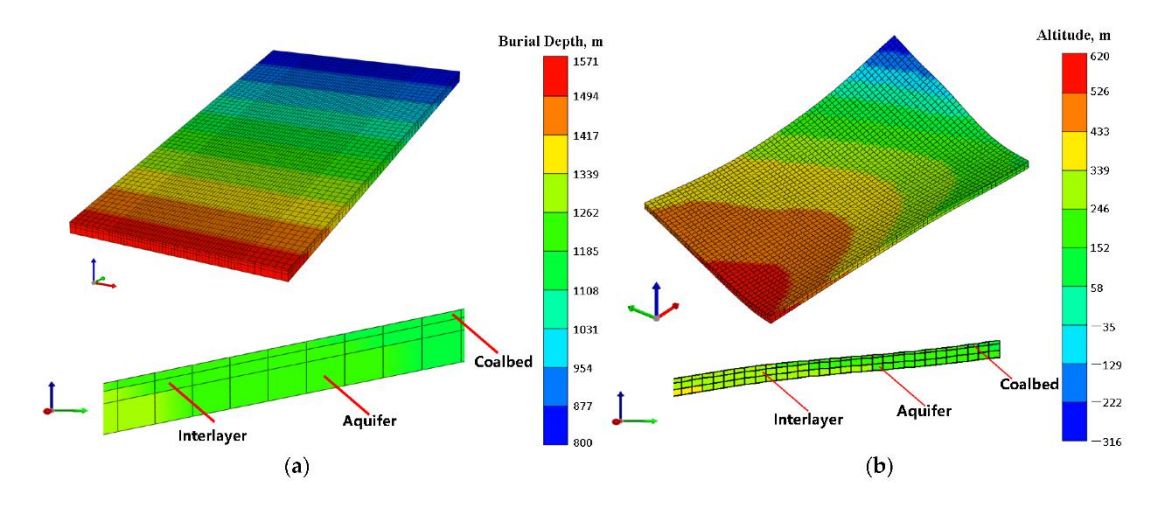


Fig. 5. Surface subsidence contour of underground coal gasification.

When the breadth of the protective coal rib is calibrated to 12 meters, the apex of the disparity in the surface subsidence ratio between shaftless dual-channel underground coal gasification (SDUCG) and strip mining is quantified at 0.028, accentuating a markedly pronounced divergence. With the protective coal rib's breadth set at 12 meters, its load-bearing capability is insufficient to uphold the equilibrium of the overlaying stratum, instigating structural instability; upon amplifying the protective coal rib's breadth to 20 meters and the expanse of the combustion void sector to 28 meters, the zenith discrepancy in the surface subsidence ratio between the dual extraction methodologies narrows to 0.015; moreover, the zenith disparity is merely 0.004, indicating that the 20-meter-wide protective coal rib can no longer effectively prop up the superimposed stratum; when the protective coal rib's breadth is extended to 28 meters or 36 meters, and the expanse of the combustion void sector is maintained at 28 meters, the zenith deviation of the surface subsidence ratio between SDUCG and strip mining is 0.01, with the remainder being 0.01 [17]. The zenith disparity in the ground subsidence ratios is merely 0.003; thus, when the protective coal rib is in a state of instability, the disparity in the zenith surface subsidence ratios of the dual extraction paradigms is 0.028; when the protective coal rib is stable and the expanse of the combustion sector is inferior to 28 meters, the zenith disparity in the surface subsidence ratios of SDUCG and strip mining is merely 0.004, with the surface subsidence ratios of the dual being virtually identical; when the protective coal rib is unstable, the zenith deviation of the lateral displacement ratios of SDUCG and strip mining is 0.01; under the condition that the protective coal rib is stable, the zenith deviation of the lateral displacement ratios of the dual is merely 0.006. In summation, when the expanse of the gas-gap sector does not surpass 20 meters and the architecture of the isolated coal rib is stable, the disparity in the surface subsidence ratio and lateral displacement ratio between SDUCG and strip mining is negligible, 0.004 and 0.006 respectively, which are fundamentally synchronized. This elucidates that under akin geological extraction conditions and recovery rate backdrop, the surface subsidence ratio and lateral displacement ratio of SDUCG can be approximately deemed equivalent to the surface subsidence ratio and lateral displacement ratio of strip mining under identical conditions [18]. The tangent value of the primary impact angle can efficaciously delineate the boundary of the surface subsidence region. Therefore, this chapter extracts the surface subsidence region boundary of SDUCG and strip mining under varying gasification residue ratios for comparative scrutiny based on the numerical simulation outcomes, with the objective of probing the fluctuation characteristics of the tangent value of the primary impact angle. This document exclusively showcases the comparative illustration of the surface subsidence region boundary of the dual extraction methodologies under distinct protective coal rib breadth scenarios when the expanse of the gas-gap sector is 20 meters. For specifics, kindly refer to Figure 6.

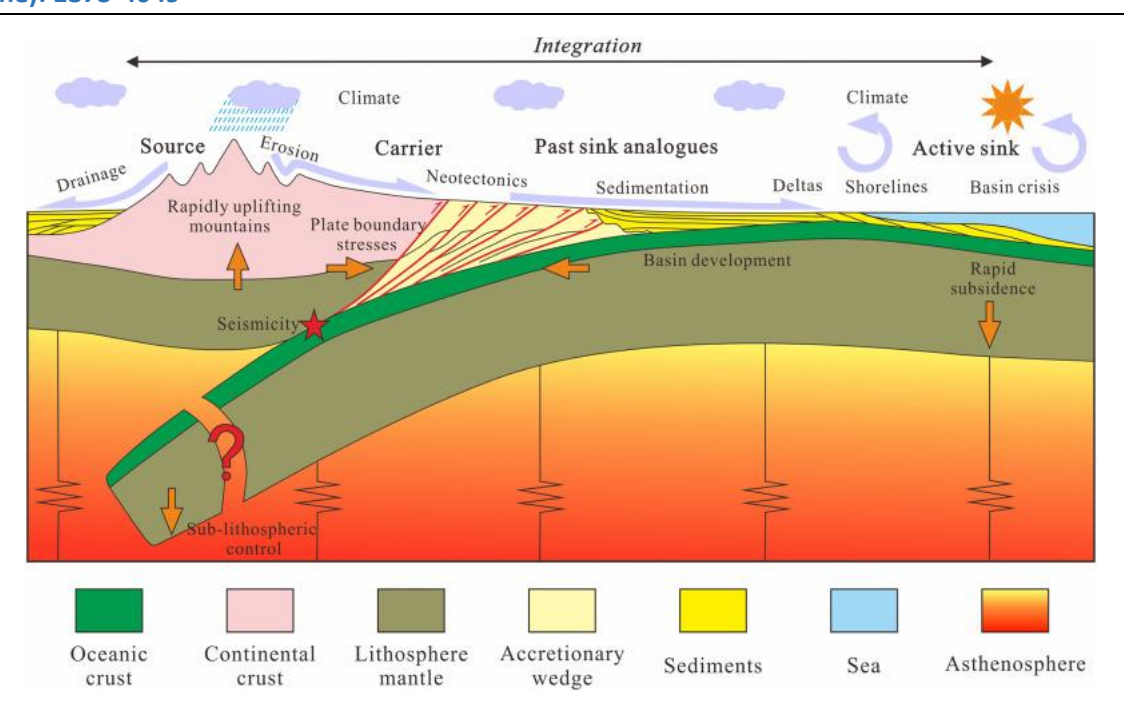


Fig. 6. Comparison of surface subsidence basin boundaries

When the breadth of the protective coal rib is calibrated to 12 meters, the zenith deviation of the surface subsidence basin demarcation between shaftless dual-channel underground coal gasification (SDUCG) and strip mining is approximately 22 meters, showcasing a relatively pronounced disparity; upon expanding the protective coal rib's breadth to 20 meters [19], the zenith deviation of the surface subsidence basin demarcation between the dual is condensed to roughly 16 meters; when the protective coal rib's breadth is augmented to 28 meters, the zenith deviation of the surface subsidence basin demarcation is roughly 15 meters; when the protective coal rib's breadth is magnified to 36 meters, the zenith discrepancy between the surface subsidence basin demarcations of the dual is roughly 16 meters. Hence, when the protective coal rib architecture is stable, the zenith deviation of the surface subsidence basin demarcation between SDUCG and strip mining is approximately 16 meters, which is fundamentally synchronous, and the primary impact angle tangent value of strip mining under identical conditions can be approximately adopted. Subsequent to the gasification operation based on temperature field distribution traits, although the stratum overhead the combustion sector is influenced by high temperatures, its influence radius is confined, and the coal seams within the study area are nearly horizontally oriented [20]. The mining impact propagation angle is predominantly determined by the traits of the overlaying stratum and the dip angle of the coal seam. Therefore, the mining impact propagation angle can be selected under identical conditions as strip mining. The inflection point offset distance is predominantly influenced by the traits of the stratum. Given the limited influence radius of high temperatures, the inflection point offset distance can also be utilized under identical conditions as strip mining. When the protective coal rib persists in a stable state and the prediction accuracy prerequisites are relatively lenient, the surface subsidence prediction parameters of SDUCG can be selected from the subsidence prediction parameters under identical conditions as strip mining [21].

To further probe the interrelation between the surface subsidence pattern and the gasification retention ratio of the combustion sector during the SDUCG process, the paper utilized ANSYS to construct the corresponding numerical model and conducted simulation scrutiny in FLAC3D software. By extracting the simulation data of the surface subsidence value within the numerical model, the correlation chart between the breadth of the combustion sector and the breadth of the protective coal rib and the surface subsidence value was illustrated, as depicted in Figure 7. The paper further delineated the fluctuation of the zenith surface subsidence under varying gasification retention ratios, as illustrated in Figure 8. This is to comprehensively scrutinize the impact of the gasification retention ratio of the combustion sector on the surface subsidence law of the wellless dual-channel underground coal gasification.

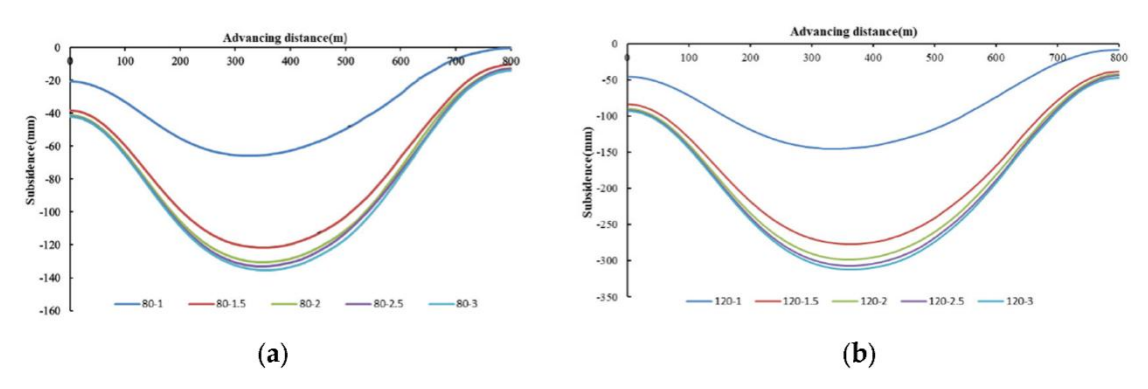


Fig.7. Relationship between the width of the isolated coal pillar and the surface subsidence curve

When the breadth of the combustion void sector is calibrated at 12 meters, the surface subsidence value exhibits diverse degrees of diminution with the amplification of the breadth of the segregated coal rib, and the diminution magnitude illustrates a tendency to progressively stabilize. When the breadth of the segregated coal rib gradually escalates from 12 meters to 20 meters, 28 meters, and 36 meters, the zenith surface subsidence values of the two contiguous models are reduced by 11 millimeters, 2 millimeters, and 2 millimeters respectively [22]; when the breadth of the combustion void sector is stabilized at 20 meters, the breadth of the segregated coal rib amplifies from 12 meters to 20 meters, 28 meters, and 36 meters sequentially, and the zenith surface subsidence values of the two contiguous models are reduced by 16 millimeters, 5 millimeters, and 5 millimeters respectively; when the breadth of the combustion void sector is stabilized at 28 meters, the breadth of the segregated coal rib amplifies from 12 meters to 20 meters, 28 meters, and 36 meters sequentially, and the zenith surface subsidence values of the two contiguous models are reduced by 48 millimeters, 24 millimeters, and 19 millimeters respectively. All surface settlement curves are distributed in an inverted V configuration, and with the enlargement of the breadth of the isolation coal rib, the surface settlement values dwindle to diverse extents [23]. The magnitude of the decrease progressively dwindles with the enlargement of the breadth of the isolation coal rib and inclines toward a plateau.

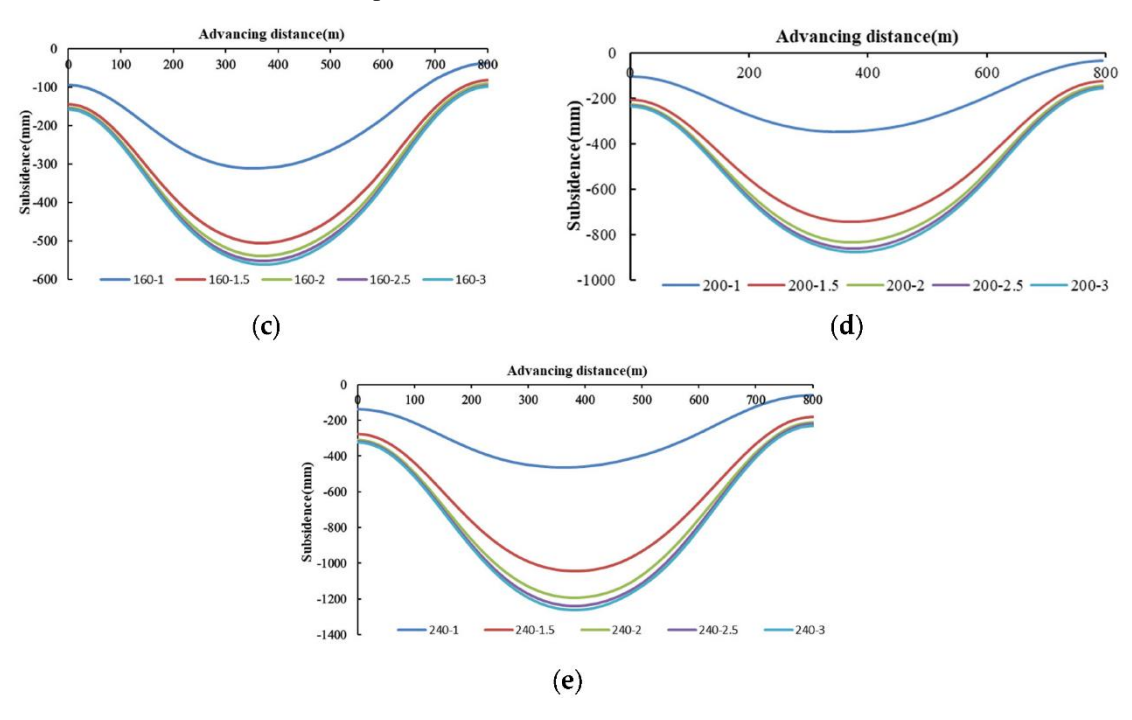


Fig. 8. Changes in the maximum surface subsidence under different gasification retention ratios

A thorough perusal of Figure 8 elucidates that with the augmentation of the combustion-gap sector's breadth, the zenith surface subsidence value has escalated to diverse extents, and its ascent becomes more pronounced with the amplification of the combustion-gap sector's breadth; the surface subsidence curve metamorphoses from a mild shape to an approximate inverted V configuration [24]. When the breadth of the protective coal rib is anchored at 12 meters, the breadth of the combustion sector progressively amplifies from 12 meters to 20 meters and 28 meters, and the zenith surface subsidence values of the two contiguous models swell by 44 millimeters and 124 millimeters respectively; when the breadth of the protective coal rib is

anchored at 20 meters, the breadth of the combustion sector progressively amplifies from 12 meters to 20 meters and 28 meters, and the zenith surface subsidence values of the two contiguous models swell by 42 millimeters and 92 millimeters respectively; when the breadth of the protective coal rib is anchored at 28 meters, the breadth of the combustion sector progressively amplifies from 12 meters to 20 meters and 28 meters, and the zenith surface subsidence values of the two contiguous models swell by 36 millimeters and 73 millimeters respectively; when the breadth of the protective coal rib is anchored at 36 meters, the breadth of the combustion sector progressively amplifies from 12 meters to 20 meters and 28 meters, and the zenith surface subsidence values of the two contiguous models swell by 32 millimeters and 59 millimeters respectively.

CONCLUSION

This study focuses on the problem of surface subsidence caused by coal mining. By constructing a multi-physical coupling model and combining Bertalanffy time function, the accurate prediction and effective control of surface subsidence are realized. The results show that the multi-physical coupling model can comprehensively consider the interaction of stress, fluid, temperature and other physical fields in the mining process, and significantly improve the accuracy of prediction. The introduction of Bertalanffy time function further improves the prediction ability of the model, and makes the prediction error of surface subsidence controlled within a reasonable range, which provides powerful data support for coal mining decision-making. In addition, by optimizing the mining strategy, the extent of surface subsidence is effectively controlled, the impact on the ecological environment is reduced, and the harmonious coexistence of mining activities and environmental protection is realized. This study provides theoretical basis and technical guidance for the sustainable development of the coal industry, and has important practical significance and application value for promoting the progress of green mining technology, protecting the ecological environment and promoting the healthy and stable development of the coal industry.

REFERENCES

- [1] Li, L., Liu, D., Cai, Y., Wang, Y., & Jia, Q. (2020). Coal structure and its implications for coalbed methane exploitation: a review. Energy & Fuels, 35(1), 86-110.
- [2] Vervoort, A. (2020). Long-term impact of coal mining on surface movement: Residual subsidence versus uplift. Min Rep Glückauf, 156(2), 136-141.
- [3] Zhe, W. A. N. G., Jie, L., Tengfei, H., & Yongchao, W. E. I. (2022). Influence of high temperature on surrounding rock damage of underground coal gasification. Journal of China Coal Society, 47(6), 2270-2278.
- [4] Wang, Z. H., Wu, S. X., Li, J. L., Sun, W. C., Wang, Z. F., & Liu, P. J. (2023). Surface subsidence and its reclamation of a coal mine locating at the high groundwater table, China. International Journal of Environmental Science and Technology, 20(12), 13635-13654.
- [5] Zhang, B., Liang, Y., Zou, Q., Chen, Z., Kong, F., & Ding, L. (2022). Evaluation of surface subsidence due to inclined coal seam mining: A case study in the 1930 Coal Mine, China. Natural Resources Research, 31(6), 3303-3317.
- [6] Li, G., Hu, Z., Yuan, D., Li, P., Feng, Z., He, Y., & Wang, W. (2022). A new approach to increased land reclamation rate in a coal mining subsidence area: A case-study of Guqiao Coal Mine, China. Land Degradation & Development, 33(6), 866-880.
- [7] Marino, G. G., Zamiran, S., & Almiron, F. (2022). An Overview of Chimney Subsidence Above Coal Mines. Geotechnical and Geological Engineering, 40(12), 5701-5715.
- [8] Zhen-qi, H. U., & Dong-zhu, Y. U. A. N. (2021). Research on several fundamental issues of coal mining subsidence control in plain coal mining area of the Lower Yellow River. Journal of China Coal Society, 46(5), 1392-1403.
- [9] Gang, C., Qiong, W., & Ming, L. X. (2020). Prediction of surface subsidence due to mining. Integrated Ferroelectrics, 209(1), 76-85.
- [10] Liang, Y. U. A. N. (2021). Research progress of mining response and disaster prevention and control in deep coal mines. Journal of China Coal Society, 46(3), 716-725.
- [11] Chi, S., Wang, L., Yu, X., Lv, W., & Fang, X. (2021). Research on dynamic prediction model of surface subsidence in mining areas with thick unconsolidated layers. Energy Exploration & Exploitation, 39(3), 927-943.
- [12] Zhao, J., Song, S., Zhang, K., Li, X., Zheng, X., Wang, Y., & Ku, G. (2023). An investigation into the disturbance effects of coal mining on groundwater and surface ecosystems. Environmental Geochemistry and Health, 45(10), 7011-7031.
- [13] Dang, V. K., Nguyen, T. D., Dao, N. H., Duong, T. L., Dinh, X. V., & Weber, C. (2021). Land subsidence induced by underground coal mining at Quang Ninh, Vietnam: Persistent scatterer interferometric synthetic aperture radar observation using Sentinel-1 data. International Journal of Remote Sensing, 42(9), 3563-3582.
- [14] Ye, D., Liu, G., Gao, F., Xu, R., & Yue, F. (2021). A multi-field coupling model of gas flow in fractured coal seam. Advances in Geo-Energy Research, 5(1), 104-118.

- [15] Zhang, J., Li, B., Liu, Y., Li, P., Fu, J., Chen, L., & Ding, P. (2022). Dynamic multifield coupling model of gas drainage and a new remedy method for borehole leakage. Acta Geotechnica, 17(10), 4699-4715.
- [16] Jahanmiri, S., & Noorian-Bidgoli, M. (2024). Land subsidence prediction in coal mining using machine learning models and optimization techniques. Environmental Science and Pollution Research, 31(22), 31942-31966.
- [17] Zou, J., Zhang, R., Zhou, F., & Zhang, X. (2023). Hazardous area reconstruction and law analysis of coal spontaneous combustion and gas coupling disasters in goaf based on DEM-CFD. Acs Omega, 8(2), 2685-2697.
- [18] LI, B., & WEI, G. (2020). Numerical simulation of thermal-fluid-solid coupling of the flow dominance of coal under different temperature conditions. Coal Science and Technology, 48(11), 141-146.
- [19] YAN, B. Q., REN, F. H., CAI, M. F., GUO, Q. F., & QIAO, C. (2020). A review of the research on physical and mechanical properties and constitutive model of rock under THMC multi-field coupling. Chinese Journal of Engineering, 42(11), 1389-1399.
- [20] Liang, W., Yan, J., Zhang, B., & Hou, D. (2021). Review on coal bed methane recovery theory and technology: recent progress and perspectives. Energy & Fuels, 35(6), 4633-4643.
- [21] Fan, C., Yang, L., Sun, H., Luo, M., Zhou, L., Yang, Z., & Li, S. (2023). Recent advances and perspectives of CO2-enhanced coalbed methane: experimental, modeling, and technological development. Energy & Fuels, 37(5), 3371-3412.
- [22] Liu, X., Fan, D., Tan, Y., Ning, J., Song, S., Wang, H., & Li, X. (2021). New detecting method on the connecting fractured zone above the coal face and a case study. Rock Mechanics and Rock Engineering, 54(8), 4379-4391.
- [23] Zhaofeng, W. A. N. G., Long, W. A. N. G., Jiaxin, D. O. N. G., & Qiao, W. A. N. G. (2021). Simulation on the temperature evolution law of coal containing gas in the freezing coring process. Journal of China Coal Society, 46(1), 199-210.
- [24] Huang, Q., Du, J., Chen, J., & He, Y. (2021). Coupling control on pillar stress concentration and surface cracks in shallow multi-seam mining. International Journal of Mining Science and Technology, 31(1), 95-101.